Specific Interactions of the L10(L12)$_4$ Ribosomal Protein Complex with mRNA, rRNA, and L11[†]

James R. Iben[‡,§,||] and David E. Draper*[,‡,⊥]

Department of Biophysics, Program in Molecular and Computational Biophysics, and Department of Chemistry, Johns Hopkins University, Baltimore, Maryland 21218

Received September 8, 2007; Revised Manuscript Received December 19, 2007

ABSTRACT: Large ribosomal subunit proteins L10 and L12 form a pentameric protein complex, L10(L12)$_4$, that is intimately involved in the ribosome elongation cycle. Its contacts with rRNA or other ribosomal proteins have been only partially resolved by crystallography. In *Escherichia coli*, L10 and L12 are encoded from a single operon for which L10(L12)$_4$ is a translational repressor that recognizes a secondary structure in the mRNA leader. In this study, L10(L12)$_4$ was expressed from the moderate thermophile *Bacillus stearothermophilus* to quantitatively compare strategies for binding of the complex to mRNA and ribosome targets. The minimal mRNA recognition structure is widely distributed among bacteria and has the potential to form a kink−turn structure similar to one identified in the rRNA as part of the L10(L12)$_4$ binding site. Mutations in equivalent positions between the two sequences have similar effects on L10(L12)$_4$−RNA binding affinity and identify the kink−turn motif and a loop AA sequence as important recognition elements. In contrast to the larger rRNA structure, the mRNA apparently positions the kink−turn motif and loop for protein recognition without the benefit of Mg^{2+}-dependent tertiary structure. The mRNA and rRNA fragments bind L10(L12)$_4$ with similar affinity ($\sim 10^8$ M^{-1}), but fluorescence binding studies show that a nearby protein in the ribosome, L11, enhances L10(L12)$_4$ binding ~100-fold. Thus, mRNA and ribosome targets use similar RNA features, held in different structural contexts, to recognize L10(L12)$_4$, and the ribosome ensures the saturation of its L10(L12)$_4$ binding site by means of an additional protein–protein interaction.

A number of ribosomal proteins regulate their own expression, and sometimes that of other ribosomal proteins as well. Though these autoregulatory proteins function by a variety of mechanisms at the levels of translation, transcription, and RNA processing, in all cases the protein recognizes and binds an mRNA target site (*1–7*). Autoregulatory ribosomal proteins are thus unusual systems in which one protein and two RNA structures have coevolved so that the protein takes on two different functional roles in different contexts. Comparative studies of the respective mRNA− and rRNA−protein complexes can be informative on several levels, including questions of recognition (are the two RNA structures and recognition strategies necessarily the same) and function (do ribosomal and regulatory roles require different characteristics of the two complexes).

In this work, we compare the mRNA and rRNA recognition sites of an unusual ribosomal protein complex, L10(L12)$_4$. Although all other ribosomal proteins are present on the ribosome in a single copy and most interact only with the rRNA, L12 binds solely to protein L10, dimerizes readily, and is present in four copies in most ribosomes [six copies are present in some bacteria (*8*)]. This pentameric complex forms a prominent stalk on the surface of the large subunit (*9, 10*), which, together with L11, L11-associated RNA, and the sarcin−ricin loop RNA, is involved in binding elongation factors to the ribosome (*11* and references therein). Although most of the ribosome structure is now known at atomic resolution (*12, 13*), details of the interactions taking place in the functionally important region containing L11, L10(L12)$_4$, and rRNA still remain to be resolved. Only in the *Haloarcula marismortui* large subunit crystal structure has a portion of L10 been observed (Figure 1A) (*14*), and L12 is not seen in any ribosome crystal structures, presumably because of inherent flexibility of L12 and the associated RNA region. The crystal structures of portions of L12 and a thermophilic L10(L12)$_6$ complex have been determined and modeled into the ribosome structure (*8*).

E. coli L10(L12)$_4$ is a translational repressor of the operon encoding its genes and binds to a structure upstream of the L10 gene initiation codon (Figure 1C) (*15, 16*). The mRNA structure potentially contains a kink−turn motif (*17*), an internal loop structural motif also identified as an L10 recognition feature in the rRNA (*14, 17, 18*). It is not known whether the kink−turn motif is sufficient for L10−RNA recognition in either mRNA or rRNA.

In this study, we set out to systematically define the features recognized by L10(L12)$_4$ in both the ribosome and mRNA targets. We first defined a minimal mRNA binding site by comparative analysis of bacterial mRNA sequences.

[†] This work was supported by NIH Grant R37-GM29048.

* Corresponding author. E-mail: draper@jhu.edu.
[‡] Department of Biophysics.
[§] Program in Molecular and Computational Biophysics.
[||] Present address: National Institute of Child Health and Human Development, National Institutes of Health, 6 Center Dr., 6A03, Bethesda, MD 20892.
[⊥] Department of Chemistry.

10.1021/bi701838y CCC: $40.75
Published on Web 02/05/2008

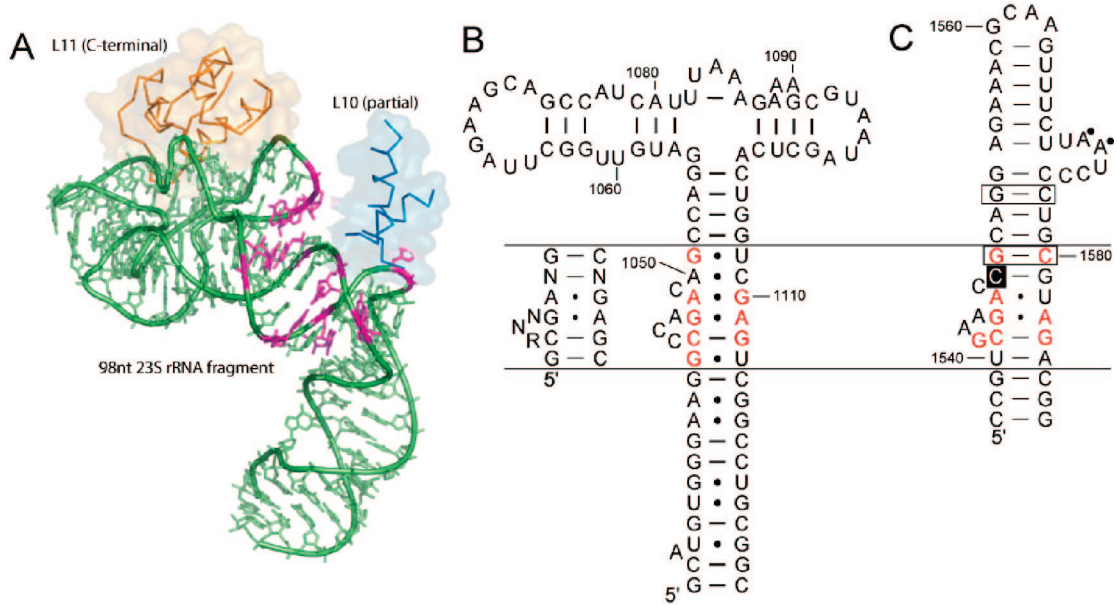

FIGURE 1: Binding sites for L10(L12)$_4$ in ribosomal and mRNAs. (A) The large subunit RNA corresponding to nucleotides 1030–1124 (*Escherichia coli* numbering) as resolved from the *H. marismortui* (*Hma*) 50S ribosomal subunit [PDB entry 1S72 (*57*)] is colored green. The L11 C-terminal domain is colored orange, and the resolved portion of L10 is colored blue. Nucleotides mutated in this study (Figure 3) are colored magenta. (B) Secondary structure of *E. coli* large subunit RNA nucleotides 1030–1124, and the consensus structure of the kink−turn motif (*17*). rRNA nucleotides corresponding to the kink−turn consensus are colored red. (C) Segment of the *E. coli rplA-rplJ* intercistronic region containing the putative L10(L12)$_4$ binding site. Nucleotides colored red correspond to the kink−turn consensus. Base pairing of the boxed nucleotides is necessary for translational regulation (*43*); mutation of C1548 (black box) to U abolishes L10(L12)$_4$ binding in vitro (*16*), and two A residues (black dots) are protected from reaction with DMS by L10(L12)$_4$ (*40*). The *rplJ* AUG codon begins at position 1720.

In measurements of L10(L12)$_4$ binding to a series of mutants in both mRNA and rRNA fragments, we found a high degree of similarity in that two features, the kink−turn motif and an AA loop sequence, contribute about the same free energy to L10(L12)$_4$ recognition in both RNAs. However, the two RNAs must use different strategies to position these features for protein recognition, the rRNA relying on a Mg^{2+}-dependent tertiary structure not present in the mRNA. In addition, we find that a cooperative interaction between L10(L12)$_4$ and a nearby protein, L11, enhances the binding affinity of L10(L12)$_4$ for ribosomes. Assembly of the ribosomal domain thus relies on a network of interactions among L11, L10, L12, and an RNA surface to form an extremely stable complex; L10(L12)$_4$ recognizes similar RNA features in its regulatory role, though the overall structural context of the mRNA site is different from that of the rRNA site.

MATERIALS AND METHODS

Cloning of the Genes for Bst[1] *L10 and L12.* The amino acid sequence of *Bacillus stearothermophilus* (*Bst*) L12 is known (*19*), but the sequence of L10 is not available. As the L10 gene is located between L1 and L12 in most bacterial genomes, primers based on the gene sequence of L1 (*20*) and the N-terminus of L12 were used to amplify genomic *Bst* DNA. After sequencing, the L10 gene was found at the expected position within the amplified DNA. In a search of genomic bacterial gene sequences, it was found that the *Bst* L10 sequence differs by only one amino acid from that of the closely related *Geobacillus kaustophilus*, by substitution of a valine for an isoleucine residue at position 154. The genes encoding *Bst* L10 and L12 were PCR-amplified from prepared genomic DNA using primers designed to introduce an *Nde*I restriction site at the gene initiation codon and a *Bam*HI restriction site just downstream of the termination codon. Each of the amplified genes was ligated into the pET15b vector (*21*) (Invitrogen). Restriction digests and DNA sequencing verified the presence of the intact inserts in the pET15b constructs, now encoding either L10 (pET15bL10f) or L12 (pET15bL12) as N-terminal (His)$_6$-tagged proteins. Since these clones were made, Shcherbakov et al. (*22*) have also reported the cloning and expression of L10 and L12 from the synonymous *Geobacillus stearothermophilus*.

Ribosomal Protein Purification. Plasmid pET15bL10f was transformed into competent BL21(DE3) *Escherichia coli* cells and plated on ampicillin-containing LB agar plates. Individual colonies were selected and grown in LB medium (*23*), induced with IPTG, and harvested. The cells were then resuspended in 25 mL of lysis buffer [0.5 M NaCl and 20 mM Tris (pH 7.9)] and lysed with a French press. Spinning the lysate in a Beckman JA-20 rotor for 45 min at 13K rpm pelleted the cell debris containing L10 in inclusion bodies. The supernatant was decanted, and to further remove soluble proteins, the pellet was resuspended in 30 mL of lysis buffer and then spun for 25 min at 8K rpm. The pellet was then resuspended by pipet in 25 mL of lysis buffer containing 6 M urea and 5 mM imidazole (binding buffer), and spun at 13K rpm for 30 min. The supernatant was loaded onto a column containing 10 mL of packed His-Bind resin (Novagen), prepared and charged as indicated, and then eluted with binding buffer containing 100 mM imidazole. Fractions containing His-tagged L10 (as detected by SDS gel electro-

[1] Abbreviations: *Bst*, *Bacillus stearothermophilus*; *Hma*, *Haloarcula marismortui*.

phoresis) were combined and dialyzed using SpectraPor dialysis tubing (8 kDa cutoff; Spectrum) into 30 mM Tris (pH 7.6), 200 mM KCl, and 3.5 M urea. The concentration of the protein was determined using a calculated extinction coefficient (*24*) at 230 nm of 60700 M^{-1} cm^{-1}.

To prepare *Bst* L12, cells transformed with pET15bL12 were grown, harvested, and lysed as described for L10. After centrifugation of the lysate, the protein remained in the supernatant, which was purified on His-Bind resin. Urea was omitted from binding buffer, and the column was eluted with buffers containing increasing concentrations of imidazole until L12 was eluted in buffer with 100 mM imidazole. The eluted protein was dialyzed into 20 mM sodium acetate (pH 5.2) (buffer A). The sample, following centrifugation for 45 min at 13K rpm, was then loaded over a TSK-SP-5PW cation exchange column (Bio-Rad) and eluted with a gradient with an increasing percentage of buffer B (buffer A with 1 M NaCl). The peak fractions (detected by absorbance at 229 nm) were combined and dialyzed into 30 mM Tris (pH 7.6) and 175 mM KCl. The concentration of the protein was determined using a calculated extinction coefficient (*24*) at 230 nm of 39800 M^{-1} cm^{-1}.

Overexpression and purification of *Bst* L11 and its C-terminal domain, L11-C76, have been described previously (*20, 25*).

Preparation of the L10(L12)$_4$ Complex. L10 was diluted into buffer to obtain (final concentrations) approximately 14 μM protein in 20 mM Tris (pH 8.4), 150 mM NaCl, 2.5 mM $CaCl_2$, and 0.5 M urea; restriction-grade thrombin protease (Novagen) was added to this solution. In parallel, L12 was diluted into a solution of 20 mM Tris (pH 8.4), 150 mM NaCl, and 2.5 mM $CaCl_2$ to a final concentration of approximately 70 μM, and thrombin was added. After both protein solutions had been incubated at 37 °C for 45 min, the two were combined at a 1:4.4 L10:L12 molar ratio, and the mixture was incubated at room temperature for 2 h. The resulting solution was loaded onto an S200 (Pharmacia) size exclusion column equilibrated with 30 mM Tris (pH 7.6) and 175 mM KCl while elution was monitored at 229 nm. The purity of the complex was assessed by electrophoresis on 8% polyacrylamide gels under native conditions (*26*). Fractions containing pure complex were combined and concentrated using Centricon-50 filtration devices (Millipore).

Compilation of L10 Upstream mRNA Sequences. Using Bioperl modules (*27*), a perl script was designed to collect intergenic sequences located immediately upstream of the L10 gene from available GenBank sequences. This database of sequences was then scanned for potential kink−turn structures using the program RNAmotif (*28*), which locates secondary structures that fit user-specified criteria. The final criteria specified a 5–10 bp helix (at least 70% paired), followed by an internal loop with sequences 5′NNAGAC and 3′NA, and finally another 6–10 bp helix closing an undefined loop of 14 to 40 nucleotides. These criteria were found to be the minimum information required to reliably identify possible kink−turn motifs without accumulating a large number of extraneous irrelevant sequences and structures. The sequences identified by RNAmotif were further evaluated by mFold (*29*) for the possibility of forming thermodynamically stable secondary structures that include a kink−turn motif. The thermodynamic parameters used by mFold version 3.2 (*30*) predict that an asymmetric internal loop is more stable than a kink−turn motif; consequently, it was frequently necessary to introduce pairing constraints to find secondary structures that included potential kink−turn motifs. The mRNA leader sequences were additionally examined for sequence conservation, secondary structure, and the potential for forming stable alternative pairings with the kink−turn motif.

The kink−turn motif was identified in approximately three-fourths of the original set of upstream L10 mRNA sequences extracted from GenBank, and all of the identified structures were from the Proteobacteria or Firmicutes divisions of Eubacteria. As additional genome sequences became available, 10 additional L10 leader sequences from other bacterial divisions were examined manually (with the aid of mFold) to see if greater sequence diversity might be found. This search uncovered three additional structures, one of which (from *Thermotoga petrophila*) did not fit the original RNAmotif search criteria.

RNA Mutagenesis and Transcription. DNAs encoding 54-nucleotide mRNA or 101-nucleotide rRNA sequences under control of a T7 promoter were prepared and ligated into a pUC18 vector. The 101-nucleotide rRNA fragments were similar to those described in a study of L11−RNA recognition (*31*) but contain the U1061A mutation, which has been previously characterized as stabilizing tertiary structure in the region bound by L11 (*32*). Prior to transcription, purified plasmids were cut with either *Sma*I (mRNA fragment) or *Eco*RV (rRNA fragment). Base substitutions were made using the QuickChange PCR protocol and reagents provided from Stratagene. Successful incorporation of the base substitutions was verified by DNA sequencing. Transcription of each of these wild-type and mutant constructs was achieved as described previously (*33, 34*), using [α-^{35}S]ATP to obtain radiolabeled RNA. Transcripts were purified by electrophoresis on a 12% denaturing polyacrylamide gel. After the desired band had been excised from the gel, RNA was extracted from crushed gel slices which had previously been frozen. The extracted solution was desalted over a mini Quick Spin RNA column (Roche) as directed. Lastly, RNA was ethanol-precipitated and the pellet resuspended in buffer containing 30 mM Tris (pH 7.6), 175 mM KCl, and 3 mM $MgCl_2$.

Filter Binding Assays. Dissociation constants were determined for L10(L12)$_4$−RNA complexes essentially as described previously (*33*). Purified L10(L12)$_4$ was added at increasing concentrations to a series of siliconized microcentrifuge tubes containing a constant concentration of radioactively labeled RNA, to a final volume of 50 μL. Buffer for the assay usually consisted of 30 mM Tris (pH 7.6), 175 mM KCl, 3 mM $MgCl_2$, and 1 μM ovalbumin (Sigma). Potassium and magnesium ion concentrations were varied in several sets of assays. The combined mixture was heated to 42 °C for 15 min and then incubated on ice for 15 min; 45 μL of the sample was spotted onto a nitrocellulose filter under vacuum suction for 10 s. Filters were dried and counted on a Beckman LS6000IC scintillation counter. The total amount of radioactivity in a set of binding reactions was determined by counting a filter to which ^{35}S-labeled RNA had been applied without suction. Radioactivity counts per minute are reported as the percent RNA retained on the filter. Titration data were fit to a single-site binding isotherm, assuming L10(L12)$_4$ is in excess over RNA. Average K_d

values with standard deviations were determined from three or more assays.

UV Melting Profiles. For UV absorption experiments, RNA was transcribed (*34*) and purified over a QIAGEN-tip 100 (QIAGEN) as described previously (*35*). RNA was eluted from the tip in buffer containing 700 mM NaCl and 20% ethanol. After ethanol precipitation, RNA was resuspended in 30 mM Tris (pH 7.6), 175 mM KCl, and various $MgCl_2$ concentrations between 0 and 5 mM. The resulting sample was diluted to ~1 μM in 2 mL of equivalent buffer in quartz cuvettes, and absorbance was monitored as a function of temperature in a Cary 400Bio (Varian) UV spectrophotometer from 7 to 95 °C, scanning at a rate of 0.5 °C/min. Data were plotted as a function of derivative absorbance versus temperature, and individual melting transitions were assigned using the Global Melt Fit program (*36*).

Cooperativity between Proteins Binding rRNA. Cooperativity between L11 and L10(L12)$_4$ in binding rRNA was determined by competition for L11 between a 58mer rRNA fragment, modified with a fluorescent tag and binding only L11, and a larger rRNA fragment binding both L11 and L10(L12)$_4$. A 58mer RNA (corresponding to nucleotides 1051–1108 of the RNA shown in Figure 1B, but containing the U1061A variant) with 2′-amino-butyryl-pyrene-uridine incorporated at position 1082 was obtained from Dharmacon Research. This RNA, called py-1082 RNA, shows substantially enhanced fluorescence when the RNA is bound to L11 (*20*). Using an assay buffer described in previous studies with this RNA [10 mM MOPS (pH 7.0), 175 mM KCl, 20 mM $MgCl_2$, 1 mM DTT, 15% glycerol, and 5% DMSO], the affinity of the RNA for L11 or L11-C76 was determined by titration of the RNA with protein in an Aviv ATF105 fluorimeter (excitation at 345 nm, emission at 395 nm).

To bring the 101mer rRNA fragment affinity for L11 into a range that competes well with py-1082 RNA, a single-base pair mutation (U1058•A1080 to C•G) was introduced to yield CG101 RNA. This mutation reduces the affinity of *Bst* L11 for rRNA while having no effect on the stability of the RNA tertiary structure (E. Poliakova and D. Draper, unpublished data). The fluorescence titration was then repeated with CG101 RNA present at different stoichiometric ratios with respect to py-1082 RNA, in the presence or absence of saturating levels of L10(L12)$_4$ (5 μM). The L11 affinity for the 101mer competitor species was estimated by simulation of the competition binding curve (*20*). Similar results were obtained in three independent repetitions of each of the binding and competition titrations.

RESULTS

Expression and Purification of L10(L12)$_4$. Previous structural and thermodyamic studies of L11−RNA interactions from this laboratory have used L11 from a moderate thermophile, *B. stearothermophilus* (*Bst*). To maintain a homologous system for studying assembly of the L11−L10−L12 domain, several plasmid vectors and expression schemes for overproducing *Bst* L10 and L12 proteins were attempted. A consistently high expression level was achieved for N-terminal (His)$_6$-modified proteins (see Materials and Methods). Overexpressed L10 forms inclusion bodies; the purified protein remains soluble only in complex with L12 or in buffers containing a minimum of 3 M urea. Hence, purification of *Bst* L10 was performed in the presence of 6 M urea, diluting below 3 M urea only to accomplish cleavage of the (His)$_6$ tag by thrombin immediately prior to complex formation with L12. In titrations of L10 with L12, assayed by nondenaturing gel electrophoresis, stoichiometric formation of a complex containing a 4:1 molar ratio of L12 and L10 was observed (data not shown).

Conservation of a Potential Kink−Turn Motif in the L10 Operon mRNA Leader Sequence. In *E. coli*, adjacent operons encode ribosomal proteins L11-L1 (*rplKA*) and L10-L12 (*rplJL*) followed by subunits of RNA polymerase (*rpoBC*) (*37*). This gene organization is present in most bacteria and archaea (*38*). The L10(L12)$_4$ regulatory binding site (Figure 1C) is encoded in the intergenic region, ~160 nucleotides upstream of the L10 initiation codon (*15*). To determine what features of the putative L10 regulatory binding site have been conserved during evolution, noncoding sequences between *rplA* and *rplJ* were extracted from annotated genomes and searched for sequences potentially forming a secondary structure with the characteristics of a kink−turn motif (see Materials and Methods for details of the automated protocol and search criteria). After elimination of redundancies, a total of 39 unique sequences were recovered from a variety of bacterial genomes; they are located between 37 and 203 nucleotides upstream of the *rplJ* start codon (Tables 1 and 2 of the Supporting Information; examples are displayed in Figure 2). Although this compilation should not be considered an exhaustive survey of available genome sequences, it is clear that the regulatory motif is widespread among the bacteria. [Although translational regulation of the adjacent *rplKA* operon by L1 has been found in both eubacteria and archaea (*39*), our searches of archaeal genomes did not uncover any examples of the L10 regulatory target site.] In most cases, the sequence enclosed by the kink−turn motif is predicted to adopt a stable hairpin structure, frequently capped by a GNRA tetraloop. This hairpin positions a bulge loop containing the UUAA sequence 4 bp from the edge of the consensus kink−turn motif. Two A residues, which are protected from chemical reaction by L10(L12)$_4$ binding to the *E. coli* mRNA (*40*), are strongly conserved at the third and fourth positions of this loop. The highly conserved UAA loop at positions 1083–1085 in the rRNA (Figure 1B) is potentially located in a similar position relative to the kink−turn motif as the two conserved mRNA A residues; the relevance of this similarity for L10(L12)$_4$−RNA recognition is explored further below. In two mRNAs, the kink−turn motif encloses a potential three-helix junction similar to the secondary structure of the rRNA binding domain [*Coxiella burnetti* and *Bordetella pertussis* sequences (Figure 2A)]; the junction loop includes a UUAA sequence.

An additional characteristic of the putative L10(L12)$_4$-binding mRNA sequences is the potential for an alternative secondary structure that includes all or part of the conserved AGAC sequence of the kink−turn motif (Figure 2). The competing sequence is located either 5′ or 3′ to the kink−turn motif, depending on whether the mRNA originates from bacteria in the Proteobacteria or Firmicutes divisions, respectively, and potentially forms helices as long as 17

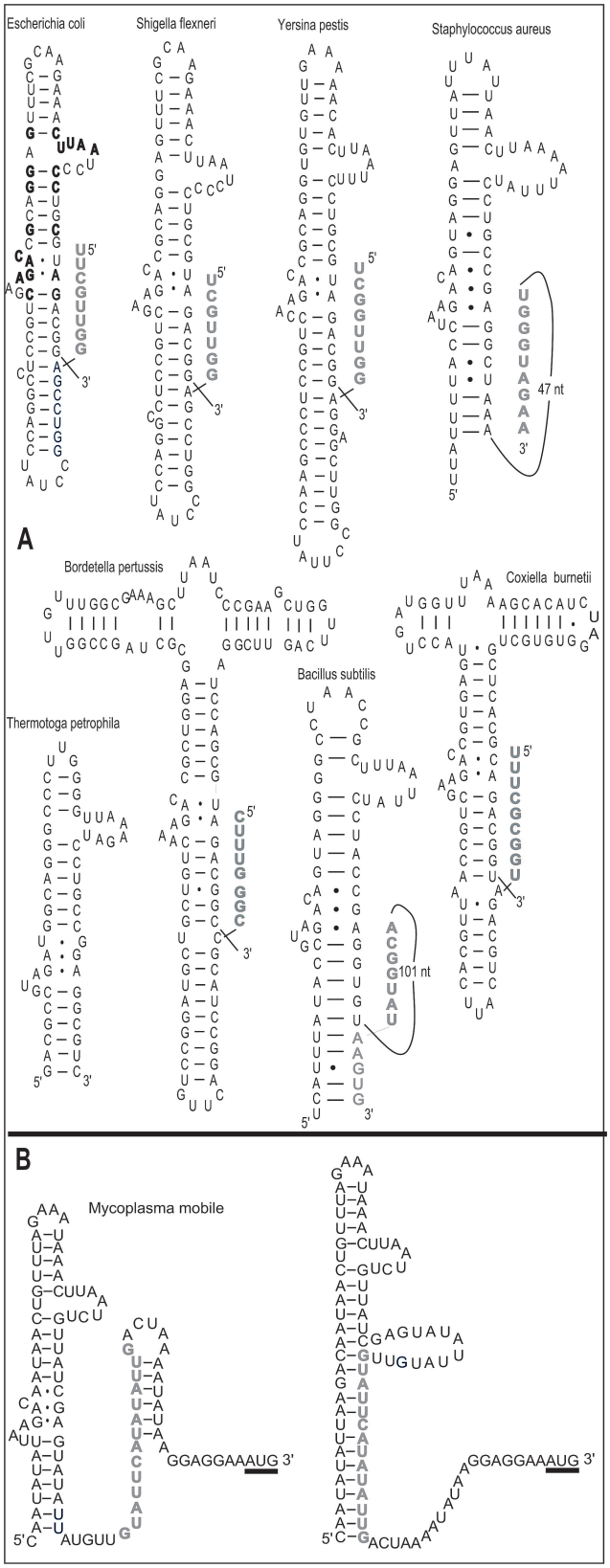

FIGURE 2: Putative L10(L12)$_4$ binding sites in bacterial mRNAs. (A) Representative kink−turn secondary structures found upstream of *rplJ* in bacterial genomes. Sequences potentially forming alternative secondary structures extending into the trinucleotide bulge of the kink−turn motif are shown in gray type. In the schematic for the *E. coli* mRNA, nucleotides in bold type are conserved in at least 37 of 39 of the aligned sequences. (B) Alternative secondary structures possible for the *Mycoplasma mobile* mRNA sequence. The *rplJ* initiation codon is at the 3′ terminus.

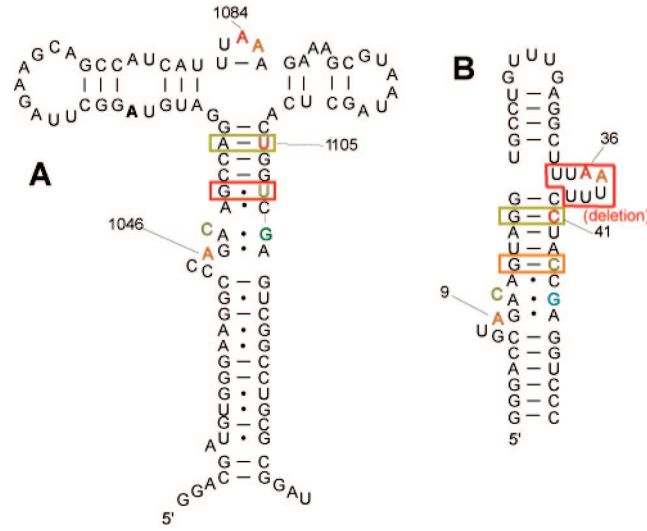

FIGURE 3: Transcribed RNAs used in filter binding assays: 101mer rRNA (A) and 54mer mRNA (B). The rRNA sequence is as shown in Figure 1B, but with the stabilizing U1061A mutation (bold) and additional nucleotides at the 5′ and 3′ termini introduced for runoff transcription. The mRNA sequence is based on the *B. stearothermophilus* L10 leader sequence; three G-C pairs at the termini replace A-U pairs in the bacterial sequence to enhance the RNA stability and enable transcription by T7 RNA polymerase. Color coding summarizes the results of binding studies with mutants (Table 1): positions with a $\Delta(\Delta G^\circ)$ for L10(L12)$_4$ binding of >3 (red), 1–2 (orange), −0.1–1 (gold), and −0.7 kcal/mol (green). Colored nucleotides refer to the effects of single-base mutations; colored boxes enclose compensatory base pair mutations, and the larger box enclosing seven mRNA nucleotides represents deletion of the bulge loop.

canonical base pairs. (*T. petrophila*, from the Thermotoga division, lacks a competing sequence.)

Comparison of Binding of L10(L12)$_4$ to mRNA and rRNA. On the basis of the analysis of putative L10(L12)$_4$ binding sites in rRNA and bacterial mRNAs, a minimal *Bst* mRNA sequence was synthesized for use in L10(L12)$_4$ binding assays (Figure 3B). As a first demonstration that this RNA represents a sufficient binding site for *Bst* L10(L12)$_4$, the formation of a single, 1:1 complex between the protein and mRNA fragment was observed in gel mobility shift experiments carried out at sufficiently high concentrations to ensure stoichiometric binding (data not shown). The affinity of the protein complex for the RNA was then determined by a filter binding assay, establishing a dissociation constant for the protein and mRNA of 21.9 ± 3.3 nM [300 mM KCl, 3 mM $MgCl_2$, and 30 mM Tris (pH 7.6)] (Figure 4). A similar dissociation constant, 31.7 ± 4.3 nM, was found for a 98-nucleotide region of 23S rRNA containing the kink−turn motif (Figure 3A), using identical solution conditions (Figure 4).

A suggestion that both the mRNA and rRNA fragments interact with L10(L12)$_4$ in similar ways comes from the salt dependences of the interactions (Figure 5A); $d(\log[K^+])/d[\log(K_d)]$ is 2.1 in both cases. Protein−nucleic acid complexes are typically weakened by an increasing level of salt because of electrostatic interactions between protein basic residues and the negatively charged nucleic acid backbone. The structure of L10 (*41*) and the occurrence of conserved basic residues in the N-terminal RNA-binding domain suggest that L10−RNA binding should also be affected by salt. A report that rRNA binding by four archaeal L10(L12)$_4$

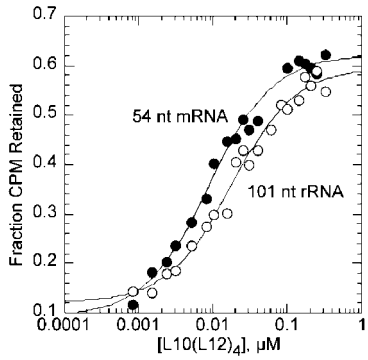

FIGURE 4: Filter binding assay of $L10(L12)_4$ associating with mRNA (●) or rRNA (○) fragments, carried out in buffer containing 30 mM Tris (pH 7.6), 300 mM KCl, 3 mM $MgCl_2$, and 1 μM ovalbumin. Dissociation constants averaged from fits of single-site binding isotherms to three independent titrations are 21.9 ± 3.3 nM (mRNA) and 31.7 ± 4.3 nM (rRNA).

complexes is essentially independent of salt is thus unexpected (*22*) and seems at odds with the more typical behavior we find for *Bst* $L10(L12)_4$.

The absence of Mg^{2+} only mildly weakened $L10(L12)_4$ recognition of the mRNA fragment ($K_d \approx 67$ nM) but rendered any protein complex with the rRNA fragment undetectable ($K_d > 400$ nM) (Figure 5B). We hypothesize that Mg^{2+} stabilizes the $L10(L12)_4$−rRNA complex indirectly, by promoting the formation of tertiary structure that positions recognition features in a favorable configuration for protein binding, and that a similar, Mg^{2+}-dependent tertiary structure is not required to form the mRNA binding site. In support of this idea, we note that the domain of nucleotides 1051–1108 of the 23S rRNA forms a compact tertiary structure which is observed as an unfolding transition in melting experiments only when Mg^{2+} is present (*34*), but that melting profiles of the mRNA fragment do not show the appearance of any new transition with the addition of Mg^{2+} (Figure 6).

$L10(L12)_4$ Recognizes Similar Features of the mRNA and rRNA Fragments. To compare the specific mRNA and rRNA features recognized by $L10(L12)_4$, variant RNAs were prepared in which the kink−turn motif, UUAA bulge loop sequence, and other conserved features were modified. The affinities of $L10(L12)_4$ for these mutant RNAs were measured by filter binding assays (results summarized in Figure 3 and Table 1).

Bases A36 and A37 of the mRNA bulged loop sequence are important for protein recognition: both bases are highly conserved (Figure 2A), and mutation of either base is strongly deleterious (Table 1 and Figure 3). These results are mirrored by the universally conserved bases A1084 and A1085 of the rRNA, whose mutation equivalently weakens $L10(L12)_4$ affinity. The possibility that the mRNA and rRNA AA sequences occupy structurally similar positions is discussed further below.

A1046 of the 23S rRNA is unstacked from the rest of the kink−turn structure and appears to be recognized by the two α-helices of L10 resolved in the *Hma* 50S subunit crystal structure (Figure 1A). Substitution of this particular nucleotide with U weakens binding of $L10(L12)_4$ to the rRNA by 1.3 kcal/mol; the equivalent mutation in the mRNA is also disruptive, weakening binding by 2.2 kcal/mol.

Ribosomal position 1110 is typically G (63%) (*42*), creating an A-G noncanonical pair within the kink−turn motif, but the corresponding mRNA position, 47, is most often U (47%), with the potential for forming an A-U pair. This position is G in both the mRNA and rRNA sequences used here (Figure 3). Its substitution with U is either neutral (mRNA) or slightly stabilizing (rRNA) for $L10(L12)_4$ binding (Table 1).

We created a set of compensatory mutations in the A1054-U1105 (rRNA) and G17-C42 (mRNA) base pairs to confirm the proposed secondary structure of the mRNA. U1105A (rRNA) and C42G (mRNA) both rendered binding by $L10(L12)_4$ undetectable. The corresponding compensatory mutations, A1054U (rRNA) and G17C (mRNA), restored binding to detectable levels, resulting in a net disruption of less than 1 kcal/mol. A set of compensatory mutations at the analogous position of the *E. coli* mRNA [G1552-C1577 (Figure 1B)] abolished or restored translational regulation in vivo (*43*).

A second set of compensatory mutations was made immediately adjacent to the kink−turn motif. Single-base substitutions U1108G (rRNA) and C45G (mRNA) destabilized $L10(L12)_4$ binding by approximately 0.7 kcal/mol in each RNA, but compensatory mutations made to restore canonical base pairing, G1051U (rRNA) and G14C (mRNA), further weakened binding of $L10(L12)_4$ to both RNAs (Table 1). This result is considered further in the Discussion.

The bulged C at position 1049 (rRNA) or C12 (mRNA) is not part of the canonical kink−turn motif (*17*), and its mutation to G has a nearly negligible effect on binding in either RNA (Table 1). However, the position is conserved as a C in the mRNA sequences (97%) and in a large fraction of bacterial rRNAs (42% C, 58% A) (*42*). Possible reasons for the conservation of the bulge are considered in the Discussion.

To ask whether any of the RNA mutations affecting $L10(L12)_4$ binding affinity may have promoted a major rearrangement of the RNA structure, thereby affecting $L10(L12)_4$ binding affinity by indirect means, UV melting experiments were performed. Each mutant RNA yielded a UV melting profile equivalent to the respective wild-type RNA, with the exception of those RNAs in which a single mutation disrupted the helix 3′ to the kink−turn motif: U1108G and U1105A (rRNA), and the corresponding C45 and C42 (mRNA) (data not shown). The double mutations that restore the possibility of base pair formation at these positions also restored the wild-type melting profile. The presence of the stabilizing U1061A mutation in all the rRNA fragments is sufficient to preserve the tertiary structure at the temperature of the binding assay, even in the presence of the destabilizing A1085U mutation (data not shown) (*32*).

Cooperative Interactions between L11 and $L10(L12)_4$. Ribosomal protein L11 binds in the distorted minor groove of the 1057–1081 helix of the rRNA (Figure 1A,B). The U1082-A1086 base pair is coaxially stacked with this helix, bringing the UAA loop (1083–1085, a U-turn structure) close to loop 2 of the protein C-terminal domain (Figure 2) (*44*). Since the A1084-A1085 base pair is required for $L10(L12)_4$ binding, there is a possibility that L10 and L11 contact each other when bound to the RNA, and a model of the L11−$L10(L12)_4$−rRNA complex supports this possibility (*8*). To investigate this potential protein–protein contact

Table 1: L10(L12)$_4$−RNA Binding Affinities[a]

101mer (rRNA)	K_d (nM)	$\Delta(\Delta G°)$ (kcal/mol)	54mer (mRNA)	K_d (nM)	T_m (°C)	$\Delta(\Delta G°)$ (kcal/mol)
wild-type	11.5 ± 2.3		wild-type	21.9 ± 3.3	76.1	
			Δ34–40	>3500	71.3	>3
A1084U	>1800	>3	A36U	>3500	75.2	>3
A1085U	222 ± 87	1.75	A37U	416 ± 117	74.3	1.74
AA1084/5UU	>1800	>3	A36/7U	>3500	75.5	>3
U1105A	>1800	>3	C41G	>3500		>3
A1054U (U1105A)	47.7 ± 3.2	0.84	G18C (C41G)	67.9 ± 12.8	71.4	0.67
U1108G	34.7 ± 7.5	0.65	C45G	79.4 ± 32.9		0.76
G1051U (U1108G)	>1800	>3	G14C (C45G)	288 ± 110	74.5	1.53
G1110U	3.39 ± .30	−0.72	G47U	18.7 ± 0.74		−0.09
A1046U	95.5 ± 6.4	1.25	A9U	850 ± 212	72.8	2.17
C1049G	20.7 ± 2.1	0.35	C12G	52.1 ± 14.7		0.51

[a] Binding constants determined by a filter binding assay at room temperature, using either 3 mM $MgCl_2$, 175 mM KCl, 30 mM Tris (pH 7.6), and 1 μM ovalbumin (101mer RNA) or the same buffer with 300 mM KCl (54mer RNA). K_d errors were calculated from three or more determinations. T_m values of 54mer RNA report the maxima of the single transition in the UV melting profile.

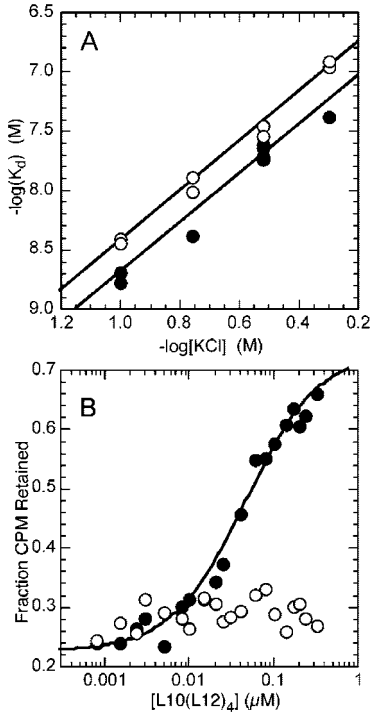

FIGURE 5: Cation dependences of L10(L12)$_4$−RNA binding affinities. (A) Monovalent salt dependence of the affinity of L10(L12)$_4$ for mRNA (●) and rRNA (○) fragments. The slope d(log[K$^+$])/d[log(K_d)] is 2.1 for each complex. (B) Affinity of L10(L12)$_4$ for mRNA (●) and rRNA (○) in the same buffer as in Figure 4. but lacking $MgCl_2$. The calculated affinity of L10(L12)$_4$ for the mRNA is 67 nM.

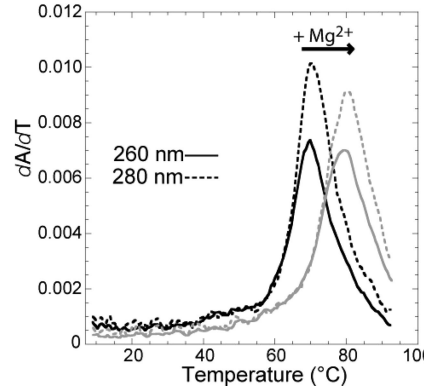

FIGURE 6: Melting profiles of the mRNA fragment, showing the effect of Mg^{2+} ion. The derivatives of absorbance at 260 (—) and 280 nm (---) with respect to temperature are shown for experiments conducted with no added Mg^{2+} (black) or 5 mM $MgCl_2$ (gray) [30 mM Tris (pH 7.6) and 175 mM KCl].

further, we looked for cooperativity between the two proteins in binding the rRNA.

To measure binding cooperativity, we first used a fluorescence assay to measure the affinity of L11 for py-1082 RNA, which corresponds to rRNA nucleotides 1051–1108 of the rRNA fragment shown in Figure 3A and has a pyrene tag attached to U1082 (*20*). This 58mer rRNA fragment lacks the kink−turn region and does not bind L10(L12)$_4$ (data not shown). In the buffer used for these titrations (see Materials and Methods), the L11−py-1082 RNA affinity is 146 ± 12 μM^{-1}. To obtain a version of the 101-nucleotide rRNA fragment with an affinity for L11 in an appropriate range for competition experiments, a base pair substitution which weakens L11 affinity by ∼10-fold without destabilizing the RNA tertiary structure was introduced (CG101 RNA; see Materials and Methods). A known ratio of CG101 RNA to py-1082 RNA was titrated with L11, and the data were compared to those from simulated titrations in which the L11 affinity for the larger, untagged RNA was varied (Figure 7A). Finally, the mixture of rRNA fragments was titrated with L11 in the presence of a saturating level of L10(L12)$_4$. This experiment showed that L10(L12)$_4$ stimulates binding of L11 to the larger rRNA fragment by a factor of ∼100 (Figure 7A). At the RNA concentrations used in these competition titrations, this stimulation factor is equivalent to the L11−L10(L12)$_4$ cooperativity factor (*20*).

The C-terminal domain of L11, L11-C76, bound py-1082 RNA with a somewhat weaker affinity (29 μM^{-1}) than did L11, as previously observed (*20*). Competition titrations using this protein fragment showed a similar cooperativity factor of ∼40 (Figure 7B). Because the relative affinities of L11 for the two RNAs used in these titrations lie close to the extremes that the experiment is able to resolve, the estimated cooperativity factor is a lower limit. Nevertheless, the effect of L10(L12)$_4$ on the apparent affinity of L11 for 101mer RNA is unambiguous and indicates that there is a high degree of cooperativity in the binding of the two proteins to rRNA.

DISCUSSION

L10(L12)$_4$ Recognition of RNA Targets. The presence of a regulatory binding site for L10(L12)$_4$ in the mRNA

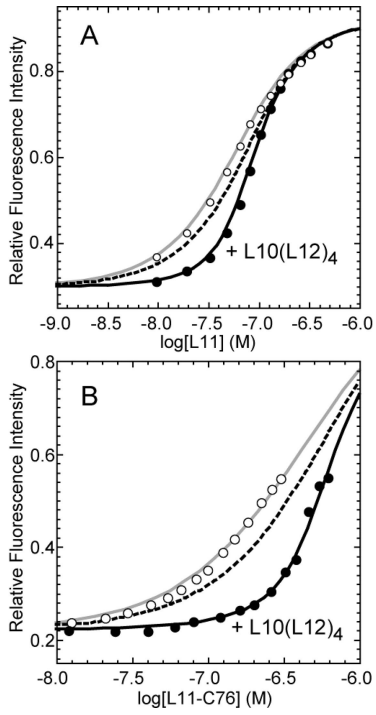

FIGURE 7: Fluorescence titrations demonstrating cooperativity of binding of L11 and L10(L12)$_4$ to rRNA. The pyrene fluorescence from a derivative of the 58mer rRNA fragment, py-1082 RNA, is being observed in the titrations (see Materials and Methods). (A) L11 titrating a 1:5 ratio of py-1082 RNA to GC 101mer rRNA fragment. The titrations were carried out in buffer containing 175 mM KCl and 20 mM $MgCl_2$, with (○) or without (●) 5 μM L10(L12)$_4$ (see Materials and Methods). Calculated curves for 1:10 (gray line), 1:1 (dashed line), and 10:1 (solid line) ratios of the L11 association constants of GC 101mer RNA to py-1082 RNA are shown. (B) Same experiment as in panel A only titrating the RNA mixture with L11-C76. The calculated curves are for 1:4 (gray line), 1:1 (dashed line), and 10:1 (solid line) ratios of protein association constants of GC 101mer RNA to py-1082 RNA.

upstream of the genes for L10 and L12 presents an opportunity to compare recognition of two different RNAs by L10(L12)$_4$. Strong evidence for similar recognition of mRNA and rRNA binding by L10(L12)$_4$ comes from the finding that $\Delta(\Delta G°)$ values for protein−RNA binding are closely parallel between two sets of mutations made in analogous positions of each RNA (Table 1). Two features of the RNA are notably implicated in L10(L12)$_4$ recognition. One feature, the kink−turn motif, was expected to form part of the rRNA recognition site, based on the partial resolution of L10 in the *Hma* large subunit crystal structure (Figure 1A) (*14*) and footprinting data (*18*). The conservation of a similar kink−turn sequence motif in the mRNA (Figure 2) and the effects of its mutation on protein binding strongly imply that L10(L12)$_4$ recognizes an essentially identical kink−turn structure in the mRNA. However, mutation of the main contact between L10 and the kink−turn motif, the bulged A1046 (rRNA) or A9 (mRNA), has a surprisingly modest effect on the L10(L12)$_4$ binding free energy [$\Delta(\Delta G°) \approx 1.2$–$2.2$ kcal/mol]. By way of comparison, mutation of a bulged A residue in the hairpin recognized by R17 coat protein is more than twice as deleterious [$\Delta(\Delta G°) > 4.7$ kcal/mol (*45*)].

The mutant RNA binding studies also suggest that a loop AA sequence is recognized by L10(L12)$_4$ in similar ways in the two RNAs. Previous mRNA footprinting experiments had shown that these two bases are protected from reaction with DMS by L10(L12)$_4$ (*40*), and re-examination of the *Hma* large subunit crystal structure by Diaconu et al. (*8*) had suggested contacts between L10 and A1084, though no hydrogen bonds with the adenine base were proposed. The recent resolution of L10 in the *Hma* 50S crystal structure also places L10 near A1084 (*41*). Our results agree, at least qualitatively, with these observations; the unexpected result is that the L10(L12)$_4$ binding affinity is much more sensitive to base changes in the loop AA sequence than in the kink−turn motif. In both mRNA and rRNA fragments, mutation of the 5′ A (A1084 or A36) reduces binding affinity below the sensitivity of the assay [$\Delta(\Delta G°) > 3$ kcal/mol], and mutation of the 3′ A (A1085 or A37) reduces affinity 20-fold [$\Delta(\Delta G°) \approx 1.7$ kcal/mol]. In the rRNA, the two A's are part of a U-turn structure (*46*) in which one side of A1084 is stacked against A1085 but otherwise exposed to solvent. Though the A1084U mutation causes a slight destabilization of the rRNA tertiary structure, the rRNA fragment should be folded at the temperature of the protein binding assays (*32*). It is therefore more likely that the A1084U variant weakens protein binding directly by affecting an L10−RNA contact, rather than indirectly by disrupting rRNA structure. As the proposed L10−rRNA model places only a valine residue near the A1084 base (*8*), the large effect of the A1084U mutation is surprising and suggests that there may be more extensive interactions of this base with L10.

Several of the binding measurements with mutant RNAs (Table 1) deserve additional comment. First, the mRNA compensatory mutation G14C/C45G did not restore L10(L12)$_4$ affinity that had been weakened by the single mutation C45G, and the analogous compensatory mutant in the rRNA (G1051U/U1108G) also bound L10(L12)$_4$ more weakly than the single-nucleotide disruption. However, a similar pair of compensatory mutations in the *E. coli* mRNA maintained translational regulation in vivo (*43*). A possible explanation for this discrepancy is that there is a neighboring Watson–Crick pair (13C/46G) in the *E. coli* mRNA but a noncanonical A·C pair in the *Bst* mRNA and rRNA fragments. The sequence context may determine what base pairs are allowed at the 14/45 mRNA helix position.

Also of interest are the effects of mutations G1110U (rRNA) and G47U (mRNA), which change an A·G pair within the kink−turn motif to an A-U pair. A slight stabilization of L10(L12)$_4$ binding is observed in the case of the rRNA variant. All four nucleotides are found at this position in both mRNA and rRNA aligned sequences, though U is the most common in the mRNA (approximately half) and G is more common (63%) in bacterial rRNAs (*42*). The affinity of L10(L12)$_4$ for the kink−turn motif is apparently weakly sensitive to the identity of this noncanonical pair.

Lastly, we note that the single-base C bulge, C1049 (rRNA) or C12 (mRNA), is not part of the consensus kink−turn motif (Figure 1B). As C1049 points away from L10 in the *Hma* ribosome crystal structure and its mutation to G only weakly reduces L10(L12)$_4$ binding affinity, it appears to be largely irrelevant to L10 recognition. This bulged C is presumably conserved in the ribosome because it hydrogen bonds to G2751 as part of a tertiary structure linking the L10−L11 binding region and a four-helix junction containing the sarcin−ricin loop. A rationalization for the strong conservation of a C bulge in the mRNA is less

apparent. In the one variant found at this position, the bulged nucleotide has been replaced by a G•U pair [*T. petrophila* (Figure 2)]; perhaps a specific distortion of the helix structure is required at this position. Alternatively, translational regulation might depend on other interactions of the mRNA structure besides those with L10(L12)$_4$.

Given the closely parallel effects of mutations in the mRNA and rRNA sites for L10(L12)$_4$, how similar might we expect the two RNA structures to be? The two kink−turn motifs must be nearly identical in structure, if not in their contacts with L10 as well, but the structural contexts of the two loop AA sequences are likely to be different. In the rRNA, the recognized UAA loop is a U-turn motif (*46*) which is highly constrained by the U1082/A1086 base pair and contained within an elaborate tertiary structure. Although a UUAA sequence is found at the 5′ end of a bulge loop in all of the mRNAs, the high variability of the 3′ part of the loop suggests that the UUAA conformation is not as tightly constrained as the UAA loop in rRNA. Our alignment of putative L10 target sites does not provide any hint that the UUAA sequence is embedded in a larger tertiary structure, and the weak effect (if any) of Mg^{2+} on the stability of the RNA or on the L10(L12)$_4$−mRNA binding affinity also argues that the UUAA-containing loop does not adopt any compact tertiary structure. It thus seems unlikely that the mRNA uses the same structural strategy to position the UUAA sequence that was used by rRNA to configure the UAA loop. The different structural contexts of the loops in the two RNAs have nevertheless evolved so that the AA sequences contribute similarly to the L10(L12)$_4$ binding free energy.

There are two ribosomal protein translational repressors for which atomic-resolution structures of both protein−rRNA and protein−mRNA target sites are available. S8 recognizes an irregular helix in both the 16S rRNA and a structure within the *spc* operon mRNA; although there are some minor sequence differences, the recognition complexes are essentially superimposable (*47*). L1−RNA recognition is a more involved story. L1 binds a large subunit rRNA structure in which a perpendicular orientation of two helices is stabilized by extensive tertiary interactions between two internal loops; L1 contacts grooves of both helices and also some of the loop bases (*48*). The mRNA target for L1 has only a single internal loop, but its flanking helices adopt a similar relative position as do the helices of the target rRNA; a similar (but less extensive) set of hydrogen bonds is also formed with the protein surface (*49*).

L1 recognition of its target sites parallels L10−RNA recognition, in that the mRNA target site is able to mimic the positioning of recognized nucleotides in the rRNA while using a less elaborate structure lacking tertiary interactions. It is not possible to decide whether the more minimalist mRNA structures represent instances of convergent evolution reproducing only the essential features of the rRNA target structure or whether [as hinted by the more rRNA-like *Bordetella* and *Coxiella*mRNA structures (Figure 2)] the rRNA structure was originally duplicated in the mRNA and later pared by natural selection to a more compact form.

Translational Repression of rplJL. In previous studies of the *E. coli* mRNA, it was suggested that binding of L10(L12)$_4$ to the upstream target site is directly coupled to changes in mRNA secondary structure that occlude the *rplJ* ribosome binding site (*16*). Direct competition between ribosomes and repressor for binding to respective "open" and "closed" ribosome binding sites occurs in other instances of translational repression, such as regulation of the R17 coat protein gene (*50*), the *spc* operon (*47*), and threonyl-tRNA synthetase (*thrS*) (*5*). Although the L10(L12)$_4$ binding site is far upstream of the *rplJ* ribosome binding site, plausible *E. coli* mRNA secondary structures were proposed which would link alternative structures at the L10 and ribosome binding sites in such a way that repressor and 30S subunit binding to the mRNA would be mutually exclusive (*16*). Some mRNA mutations which suppress translation of the *E. coli* mRNA in vivo are located between the repressor and ribosome binding sites (*51*), suggesting that the overall structure of the mRNA is important for the translational regulation mechanism. With our compilation of additional mRNA target sites, we can ask whether this proposed structural linkage between the L10(L12)$_4$ and ribosome binding sites has been conserved. In support of the existence of alternative mRNA secondary structures, most of the predicted L10 recognition sites can adopt an alternative base pairing that would disupt the kink−turn motif. However, we failed to find a consistent mechanism by which formation of the kink−turn secondary structure would promote occlusion of the translational initiation site, among either the Proteobacteria (alternative structure is formed from a sequence 5′ to the kink−turn structure) or Firmicutes (alternative sequence is 3′ to the kink−turn motif). In the mRNA structures predicted for the *M. mobile* mRNA, for instance, only an A-U rich helix just upstream of the potential secondary structure is linked to folding of the kink−turn recognition site (Figure 2B). This weak helix is unlikely to prevent translational initiation (*52*).

An alternative to a competitive mechanism for translational repression is entrapment, in which the repressor stabilizes the initiating ribosome in a state which is unable to continue translation (*53*). Evidence for a stable entrapment complex among repressor, ribosome, and mRNA has been demonstrated for two autoregulatory ribosomal proteins, S4 and S15 (*6, 7*). It may be that L10(L12)$_4$ binding to the upstream mRNA places the protein complex in a position to interfere with a ribosome bound at the mRNA initiation site. However, this suggestion does not provide a role for the apparently conserved alternative mRNA secondary structure. The actual method by which translational feedback regulation is enacted remains unclear and will require further work to elucidate.

Cooperativity and Ribosome Assembly. Mutual stimulation in the binding of L11 and L10(L12)$_4$ to a large 23S rRNA fragment was observed in early studies of these proteins (*54*). The L11 binding region of the *E. coli* rRNA used in those studies is marginally stable (*34*), and binding of either L11 or L10(L12)$_4$ induces protection in the rRNA consistent with stabilization of rRNA tertiary structure (*18*). Thus, Diaconu et al. plausibly argued that the apparent L11−L10(L12)$_4$ binding cooperativity is communicated by RNA conformational changes, rather than by the few protein–protein contacts seen in their model of the protein−rRNA complex (see the Supporting Information of ref *8*). The rRNA fragment used in our study to measure L11−L10(L12)$_4$ binding cooperativity contains the stabilizing U1061A mutation. Hydroxyl radical cleavage and melting experiments show that the L11-binding region of this variant rRNA is

completely folded under the conditions of our binding experiments (*32, 55*). We therefore argue that the ~100-fold cooperativity factor that we measure originates in contacts between L10 and L11. The recently determined crystal structure that resolves both L10 and L11 in the *Hma* ribosome finds 250 Å^2 of buried surface area between the two proteins (*41*), too small to promote formation of an L10−L11 bimolecular complex but consistent with ~100-fold cooperativity. The high degree of sequence conservation seen in the contact regions of these two proteins (*8*) also argues that the contact is relevant to ribosome function.

The affinities of the *Bst* L11 and L10(L12)$_4$ proteins for rRNA are ~10^9 (*20*) and ~10^8 M^{-1}, respectively (referenced to buffer containing 175 mM KCl at 20 °C, and the stable U1061A rRNA variant). The cooperativity between the proteins boosts these apparent affinities further. {At free protein concentrations of $>10^{-8}$ M, the average apparent binding affinity of each protein is $[100(10^9\ M^{-1})(10^8)]^{1/2} = 3 \times 10^9\ M^{-1}$.} If these affinities apply in vivo, where ribosome concentrations are on the order of 10 μM and pools of free ribosomal proteins are perhaps 0.1–1 μM (*53*), the fraction of ribosomes having both L11 and L10(L12)$_4$ bound would be in excess of 99.9%, a number that is consistent with in vivo studies estimating that only 1 in ~10^4 ribosomes in *E. coli* lacks L11 at any one time (*56*). In the absence of protein–protein cooperativity, these high saturation levels would probably not be achieved. The cooperativity between L11 and L10(L12)$_4$ is also relevant to translational repression, which depends on L10(L12)$_4$ first titrating all available ribosome binding sites before binding to mRNAs. Although the mRNA and rRNA binding affinities are comparable (Table 1), the 100-fold L10−L11 cooperativity ensures that ribosomes will effectively compete against mRNA for L10(L12)$_4$.

SUPPORTING INFORMATION AVAILABLE

Sources of L10 leader sequences containing a potential kink−turn motif (Table 1) and alignments of L10 leader sequences (Table 2). This material is available free of charge via the Internet at http://pubs.acs.org.

REFERENCES

1. Nomura, M., Gourse, R., and Baughman, G. (1984) Regulation of the Synthesis of Ribosomes and Ribosomal Components. *Annu. Rev. Biochem. 53*, 75–117.
2. Zengel, J. M., and Lindahl, L. (1990) Ribosomal protein L4 stimulates *in vitro* termination of transcription at a NusA-dependent terminator in the S10 operon leader. *Proc. Natl. Acad. Sci. U.S.A. 87*, 2675–2679.
3. Zengel, J. M., and Lindahl, L. (1994) Diverse mechanisms for regulating ribosomal protein synthesis in *Escherichia coli*. *Prog. Nucleic Acid Res. Mol. Biol. 47*, 331–370.
4. Dabeva, M. D., and Warner, J. R. (1993) Ribosomal protein L32 of *Saccharomyces cervisiae* regulates both splicing and translation of its own transcript. *J. Biol. Chem. 268*, 19669–19674.
5. Moine, H., Romby, P., Springer, M., Grunberg-Manago, M., Ebel, J. P., Ehresmann, B., and Ehresmann, C. (1990) *Escherichia coli* threonyl-tRNA synthetase and tRNA(Thr) modulate the binding of the ribosome to the translational initiation site of the thrS mRNA. *J. Mol. Biol. 216*, 299–310.
6. Philippe, C., Eyermann, F., Benard, L., Portier, C., Ehresmann, B., and Ehresmann, C. (1993) Ribosomal protein S15 from *Escherichia coli* modulates its own translation by trapping the ribosome on the mRNA initiation loading site. *Proc. Natl. Acad. Sci. U.S.A. 90*, 4394–4398.
7. Schlax, P. J., Xavier, K. A., Gluick, T. C., and Draper, D. E. (2001) Translational repression of the *Escherichia coli* alpha operon mRNA: Importance of an mRNA conformational switch and a ternary entrapment complex. *J. Biol. Chem. 276*, 38494–38501.
8. Diaconu, M., Kothe, U., Schlunzen, F., Fischer, N., Harms, J. M., Tonevitsky, A. G., Stark, H., Rodnina, M. V., and Wahl, M. C. (2005) Structural basis for the function of the ribosomal L7/12 stalk in factor binding and GTPase activation. *Cell 121*, 991–1004.
9. Agrawal, R. K., Heagle, A. B., Penczek, P., Grassucci, R. A., and Frank, J. (1999) EF-G-dependent GTP hydrolysis induces translocation accompanied by large conformational changes in the 70S ribosome. *Nat. Struct. Biol. 6*, 643–647.
10. Matadeen, R., Patwardhan, A., Gowen, B., Orlova, E. V., Pape, T., Cuff, M., Mueller, F., Brimacombe, R., and van Heel, M. (1999) The *Escherichia coli* large ribosomal subunit at 7.5 Å resolution. *Struct. Folding Des. 7*, 1575–1583.
11. Mohr, D., Wintermeyer, W., and Rodnina, M. V. (2002) GTPase activation of elongation factors Tu and G on the ribosome. *Biochemistry 41*, 12520–12528.
12. Schuwirth, B. S., Borovinskaya, M. A., Hau, C. W., Zhang, W., Vila-Sanjurjo, A., Holton, J. M., and Cate, J. H. (2005) Structures of the bacterial ribosome at 3.5 Å resolution. *Science 310*, 827–834.
13. Selmer, M., Dunham, C. M., Murphy, F. V. t., Weixlbaumer, A., Petry, S., Kelley, A. C., Weir, J. R., and Ramakrishnan, V. (2006) Structure of the 70S ribosome complexed with mRNA and tRNA. *Science 313*, 1935–1942.
14. Ban, N., Nissen, P., Hansen, J., Moore, P. B., and Steitz, T. A. (2000) The complete atomic structure of the large ribosomal subunit at 2.4 Å resolution. *Science 289*, 905–920.
15. Johnsen, M., Christensen, T., Dennis, P. P., and Fiil, N. P. (1982) Autogeneous control: Ribosomal protein L10-L12 complex binds to the leader sequence of its mRNA. *EMBO J. 1*, 999–1004.
16. Christensen, T., Johnsen, M., Fiil, N. P., and Friesen, J. D. (1984) RNA secondary structure and translation inhibition: Analysis of mutants in the *rplJ* leader. *EMBO J. 3*, 1609–1612.
17. Klein, D. J., Schmeing, T. M., Moore, P. B., and Steitz, T. A. (2001) The kink-turn: A new RNA secondary structure motif. *EMBO J. 20*, 4214–4221.
18. Egebjerg, J., Douthwaite, S. R., Liljas, A., and Garrett, R. A. (1990) Characterization of the Binding Sites of Protein L11 and the L10.(L12)$_4$ Pentameric Complex in the GTPase Domain of 23 S Ribosomal RNA from *Escherichia coli*. *J. Mol. Biol. 213*, 275–288.
19. Garland, W. G., Louie, K. A., Matheson, A. T., and Liljas, A. (1987) The complete amino acid sequence of the ribosomal 'A' protein (L12) from *Bacillus stearothermophilus*. *FEBS Lett. 220*, 43–46.
20. Bausch, S. L., Poliakova, E., and Draper, D. E. (2005) Interactions of the N-terminal domain of ribosomal protein L11 with thiostrepton and rRNA. *J. Biol. Chem. 280*, 29956–29963.
21. Studier, F. W., Rosenberg, A. H., Dunn, J. J., and Dubendorff, J. W. (1990) Use of T7 Polymerase to Direct Expression of Cloned Genes. *Methods Enzymol. 185*, 60–89.
22. Shcherbakov, D., Dontsova, M., Tribus, M., Garber, M., and Piendl, W. (2006) Stability of the 'L12 stalk' in ribosomes from mesophilic and (hyper)thermophilic Archaea and Bacteria. *Nucleic Acids Res. 34*, 5800–5814.
23. Maniatis, T., Fritsch, E. F., and Sambrook, J. (1982) *Molecular Cloning: A Laboratory Manual*, Cold Spring Harbor Laboratory Press, Plainview, NY.
24. Jensen, D. E., and von Hippel, P. H. (1976) DNA "melting" proteins. I. Effects of bovine pancreatic ribonuclease binding on the conformation and stability of DNA. *J. Biol. Chem. 251*, 7198–7214.
25. Xing, Y., and Draper, D. E. (1996) Cooperative interactions of RNA and thiostrepton antibiotic with two domains of ribosomal protein L11. *Biochemistry 35*, 1581–1588.
26. Griaznova, O., and Traut, R. R. (2000) Deletion of C-terminal residues of *Escherichia coli* ribosomal protein L10 causes the loss of binding of one L7/L12 dimer: Ribosomes with one L7/L12 dimer are active. *Biochemistry 39*, 4075–4081.
27. Stajich, J. E., Block, D., Boulez, K., Brenner, S. E., Chervitz, S. A., Dagdigian, C., Fuellen, G., Gilbert, J. G., Korf, I., Lapp, H., Lehvaslaiho, H., Matsalla, C., Mungall, C. J., Osborne, B. I., Pocock, M. R., Schattner, P., Senger, M., Stein, L. D., Stupka, E., Wilkinson, M. D., and Birney, E. (2002) The Bioperl toolkit: Perl modules for the life sciences. *Genome Res. 12*, 1611–1618.

28. Macke, T. J., Ecker, D. J., Gutell, R. R., Gautheret, D., Case, D. A., and Sampath, R. (2001) RNAMotif, an RNA secondary structure definition and search algorithm. *Nucleic Acids Res. 29*, 4724–4735.
29. Zuker, M. (2003) Mfold web server for nucleic acid folding and hybridization prediction. *Nucleic Acids Res. 31*, 3406–3415.
30. Mathews, D. H., Sabina, J., Zuker, M., and Turner, D. H. (1999) Expanded sequence dependence of thermodynamic parameters improves prediction of RNA secondary structure. *J. Mol. Biol. 288*, 911–940.
31. Ryan, P. C., Lu, M., and Draper, D. E. (1991) Recognition of the highly conserved GTPase center of 23 S ribosomal RNA by ribosomal protein L11 and the antibiotic thiostrepton. *J. Mol. Biol. 221*, 1257–1268.
32. Lu, M., and Draper, D. E. (1994) Bases defining an ammonium and magnesium ion-dependent tertiary structure within the large subunit ribosomal RNA. *J. Mol. Biol. 244*, 572–585.
33. Draper, D. E., Deckman, I. C., and Vartikar, J. V. (1988) Physical Studies of Ribosomal Protein−RNA Interactions. *Methods Enzymol. 164*, 203–220.
34. Laing, L. G., and Draper, D. E. (1994) Thermodynamics of RNA Folding in a Highly Conserved Ribosomal RNA Domain. *J. Mol. Biol. 237*, 560–576.
35. Johnson, M. L., Holt, J. M., and Ackers, G. K. (2008) Biothermodynamics. *Methods Enzymol.*, in press.
36. Draper, D. E., Bukhman, Y. V., and Gluick, T. C. (2000) Thermal Methods for the Analysis of RNA Folding Pathways, in *Current Protocols in Nucleic Acid Chemistry* (Beaucage, S. L., Bergstrom, D. E., Glick, G. D., and Jones, R. A., Eds.) Section 11.3, John Wiley & Sons, New York.
37. Post, L. E., Strycharz, G. D., Nomura, M., Lewis, H., and Dennis, P. P. (1979) Nucleotide sequence of the ribosomal protein gene cluster adjacent to the gene for RNA polymerase subunit β in *Escherichia coli*. *Proc. Natl. Acad. Sci. U.S.A. 76*, 1697–1701.
38. Shimmin, L. G., and Dennis, P. P. (1989) Characterization of the L11, L1, L10, and L12 equivalent ribosomal protein gene cluster of the halophilic archaebacterium *Halobacterium cutirubrum*. *EMBO J. 8*, 1225–1235.
39. Mayer, C., Kohrer, C., Grobner, P., and Piendl, W. (1998) MvaL1 autoregulates the synthesis of the three ribosomal proteins encoded on the MvaL1 operon of the archaeon *Methanococcus vannielii* by inhibiting its own translation before or at the formation of the first peptide bond. *Mol. Microbiol. 27*, 455–468.
40. Climie, S. C., and Friesen, J. D. (1988) In vivo and in vitro structural analysis of the rplJ mRNA leader of *Escherichia coli*. Protection by bound L10-L7/L12. *J. Biol. Chem. 263*, 15166–15175.
41. Kavran, J. M., and Steitz, T. A. (2007) Structure of the base of the L7/L12 stalk of the *Haloarcula marismortui* large ribosomal subunit: Analysis of L11 movements. *J. Mol. Biol. 371*, 1047–1059.
42. Cannone, J. J., Subramanian, S., Schnare, M. N., Collett, J. R., D'Souza, L. M., Du, Y., Feng, B., Lin, N., Madabusi, L. V., Muller, K. M., Pande, N., Shang, Z., Yu, N., and Gutell, R. R. (2002) The comparative RNA web (CRW) site: An online database of comparative sequence and structure information for ribosomal, intron, and other RNAs. *BMC Bioinf. 3*, 2.
43. Climie, S. C., and Friesen, J. D. (1987) Feedback regulation of the rplJL-rpoBC ribosomal protein operon of *Escherichia coli* requires a region of mRNA secondary structure. *J. Mol. Biol. 198*, 371–381.
44. Conn, G. L., Draper, D. E., Lattman, E. E., and Gittis, A. G. (1999) Crystal structure of a conserved ribosomal protein-RNA complex. *Science 284*, 1171–1174.
45. Romaniuk, P. J., Lowary, P., Wu, H. N., Stormo, G., and Uhlenbeck, O. C. (1987) RNA binding site of R17 coat protein. *Biochemistry 26*, 1563–1568.
46. Quigley, G. J., and Rich, A. (1976) Structural Domains of Transfer RNA Molecules. *Science 194*, 796–806.
47. Merianos, H. J., Wang, J., and Moore, P. B. (2004) The structure of a ribosomal protein S8/spc operon mRNA complex. *RNA 10*, 954–964.
48. Nikulin, A., Eliseikina, I., Tishchenko, S., Nevskaya, N., Davydova, N., Platonova, O., Piendl, W., Selmer, M., Liljas, A., Drygin, D., Zimmermann, R., Garber, M., and Nikonov, S. (2003) Structure of the L1 protuberance in the ribosome. *Nat. Struct. Biol. 10*, 104–108.
49. Nevskaya, N., Tishchenko, S., Volchkov, S., Kljashtorny, V., Nikonova, E., Nikonov, O., Nikulin, A., Kohrer, C., Piendl, W., Zimmermann, R., Stockley, P., Garber, M., and Nikonov, S. (2006) New insights into the interaction of ribosomal protein L1 with RNA. *J. Mol. Biol. 355*, 747–759.
50. Carey, J., Cameron, V., de Haseth, P. L., and Uhlenbeck, O. C. (1983) Sequence-specific interaction of R17 coat protein with its ribonucleic acid binding site. *Biochemistry 22*, 2601–2610.
51. Fiil, N. P., Friesen, J. D., Downing, W. L., and Dennis, P. P. (1980) Post-transcriptional regulatory mutants in a ribosomal protein-RNA polymerase operon of *E. coli*. *Cell 19*, 837–844.
52. de Smit, M. H., and van Duin, J. (1994) Control of Translation by mRNA Secondary Structure in *Escherichia coli*. A quantitative analysis of literature data. *J. Mol. Biol. 244*, 144–150.
53. Draper, D. E. (1987) Translational Regulation of Ribosomal Proteins in *Escherichia coli*. Molecular Mechanisms, in *Translational Regulation of Gene Expression* (Ilan, J., Ed.) pp 1–26, Plenum Press, New York.
54. Dijk, J., Garrett, R. A., and Muller, R. (1979) Studies on the binding of the ribosomal protein complex L7/12-L10 and protein L11 to the 5′-one third of 23S RNA: A functional centre of the 50S subunit. *Nucleic Acids Res. 6*, 2717–2729.
55. Conn, G. L., Gittis, A. G., Lattman, E. E., Misra, V. K., and Draper, D. E. (2002) A compact RNA tertiary structure contains a buried backbone-K^+ complex. *J. Mol. Biol. 318*, 963–973.
56. Maeder, C., Conn, G. L., and Draper, D. E. (2006) Optimization of a ribosomal structural domain by natural selection. *Biochemistry 45*, 6635–6643.
57. Klein, D. J., Moore, P. B., and Steitz, T. A. (2004) The contribution of metal ions to the structural stability of the large ribosomal subunit. *RNA 10*, 1366–1379.

BI701838Y